

---

# Analysis of spatial variability of hydraulic conductivity at field scale

N. Gupta<sup>1</sup>, R.P. Rudra<sup>2\*</sup> and G. Parkin<sup>3</sup>

<sup>1</sup>Schaeffers Consulting Engineers, 64 Jardin Drive, Concord, Ontario L4K 3P3, Canada; <sup>2</sup>School of Engineering, and <sup>3</sup>Department of Land Resources Science, University of Guelph, Guelph, Ontario N1G 2W1, Canada. \*Email: rrudra@uoguelph.ca

---

Gupta, N., Rudra, R.P. and Parkin, G. 2006. **Analysis of spatial variability of hydraulic conductivity at field scale.** Canadian Biosystems Engineering/Le génie des biosystèmes au Canada 48: 1.55 - 1.62. Hydraulic conductivity, a vital input parameter in physically based rainfall-runoff modeling approaches, determined by double ring infiltrometer and Guelph permeameter along and across the slope of a field, was analyzed using conventional statistical techniques and geo-statistical techniques such as auto-correlation, variogram, and kriging. The results confirmed that geo-statistical techniques better describe spatial variability of hydraulic conductivity than conventional statistical techniques. The hydraulic conductivity shows more spatial variability along the field slope than across the field slope. Therefore, more samples were required along the field slope than across the field slope to obtain a truly representative value of hydraulic conductivity. The results indicated that kriging produces a convenient smooth hydraulic conductivity surface, which may be helpful in the quantification of dominant runoff generation mechanisms and identification of runoff generation areas. **Keywords:** saturated hydraulic conductivity, spatial variability, spatial analysis, geostatistical analysis.

La conductivité hydraulique, une variable essentielle à considérer dans les approches de modélisation descriptive des événements précipitations - ruissellement, déterminée par l'infiltromètre à double anneaux et le perméamètre Guelph de manière longitudinale et transversale à la pente d'un champ a été analysée en utilisant des techniques statistiques conventionnelles et des techniques géostatistiques tels l'auto-corrélation, le variogramme et le krigeage. Les résultats ont confirmé que les techniques géostatistiques décrivent plus adéquatement la variabilité spatiale de la conductivité hydraulique que les techniques statistiques conventionnelles. La conductivité hydraulique démontre une plus grande variabilité spatiale longitudinalement à la pente que transversalement à la pente, d'où la nécessité d'avoir plus d'échantillons pris longitudinalement à la pente que transversalement pour obtenir une valeur réellement représentative de la conductivité hydraulique. Les résultats démontrent que le krigeage produit une surface lisse de conductivité hydraulique qui s'avère pratique et qui peut être utile dans la quantification des mécanismes de ruissellement dominants et l'identification des zones qui génèrent le ruissellement. Mots clés: conductivité hydraulique saturée, variabilité spatiale, analyse spatiale, analyse géostatistique.

## INTRODUCTION

Modeling approaches have been recognized to be the most important tool to address environmental issues such as non-point source pollution management, source water protection, and nutrient management. At present, the trend has been towards physically based models in which saturated hydraulic conductivity has been the most important parameter. The saturated hydraulic conductivity has also been recognized to be

a highly spatially variable hydraulic property and the modeling process requires estimation of representative values of this parameter for every field or sub-basin in a watershed.

Many extrinsic (e.g. traffic, vegetation, or land use) and intrinsic (e.g. soil types, pore size distribution) factors are responsible for the variation of soil physical and hydraulic properties from field to field in a watershed. Literature also indicates that the field saturated hydraulic conductivity is a more highly correlated spatially variable soil hydraulic property than other soil physical and hydraulic characteristics.

Moreover, the field saturated hydraulic conductivity ( $K_{fs}$ ), is also a very sensitive parameter for many physically based hydrologic, drainage, and non-point source pollution models (Stephens et al. 1984; Rudra et al. 1985; Jury 1989). At present, indirect methods based on particle size distribution, bulk density, and organic matter content (Rawls et al. 1982), laboratory methods (Klute 1965), and field methods (Gupta et al. 1993) are used to determine or estimate  $K_{fs}$ . Field research has shown that the  $K_{fs}$  generally exhibits log normal distribution (Nielsen et al. 1973; Willardson and Hurst 1965; Elrick et al. 1987; Jury 1989). Therefore, the central tendency of  $K_{fs}$  data can be represented better by the geometric mean than by the arithmetic mean.

Buchter et al. (1991) measured soil properties including soil-water-characteristic curves, particle size, saturated hydraulic conductivity, and bulk density along two parallel 100-m transects separated by 0.6 m and found that the parameters had a strong periodic behavior with a main cycle of 50 m. Rahman et al. (1996) examined the spatial variability of soil properties across the landscape and concluded that the geostatistical techniques provide a better description of the nature of variability in soil properties than conventional statistical techniques such as analysis of variance and regression analysis.

Mohanty et al. (1994) and Gupta et al. (1993) studied the spatial variability of hydraulic conductivity along a transit using in-situ field methods of hydraulic conductivity. Diwu et al. (1998) studied the spatial variations of hydraulic conductivity estimated by the constant head permeameter method (Klute 1965). In these experiments, the hydraulic conductivity was computed at different soil depths under tillage and no-tillage conditions and the resulting conclusion was that the field saturated hydraulic is a more highly spatially variable on the surface as compared to the subsurface. Govindaraju et al. (1995) studied the spatial structure of the soil infiltration properties

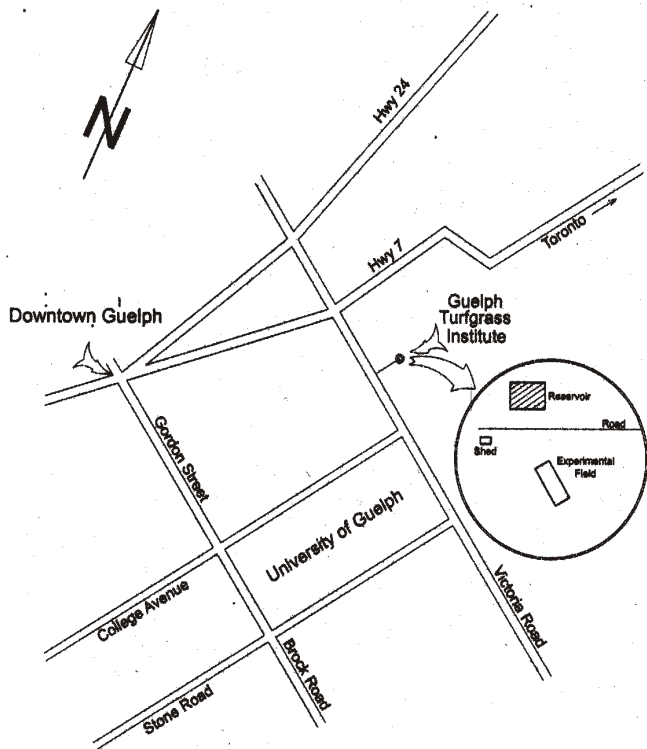


Fig. 1. Site map of the study area.

(saturated hydraulic conductivity, matrix flux potential, sorptivity, and alpha parameter) using geostatistical methods and concluded that saturated hydraulic conductivity exhibited extremely large spatial variability.

All these studies have highlighted the spatial variability of  $K_{fs}$  only in one direction, either along the slope or across the slope. Very little attention has been given to investigate the variations in  $K_{fs}$  along and across the slope. Webster and Oliver (2001) suggested that geostatistical methods can be used for description and interpretation of the spatial variability of soil physical and hydraulic properties.

The focus of this study was to investigate the spatial variations of  $K_{fs}$  along and across the slope using geostatistical methods. The fundamental aspect of the geostatistical methods is based on the idea that at some scale, the properties in the soil are in some way positively related to each other (autocorrelation) and geostatistical techniques can be applied to estimate the values of soil properties at un-sampled locations.

### DESCRIPTION OF STUDY AREA

The experimental field, 0.56 ha in area, situated at the University of Guelph campus was selected in this study (Fig. 1). The study area lies in the humid region of southwestern Ontario, with an annual precipitation of 750 - 1000 mm, 13 to 20% of which comes as snowfall during the winter period. The daily average temperature varies between 25°C and -9.6 °C. The maximum temperature occurs during the months of June to August and minimum during the months of January and February. This region experiences winter thaw during the months of January and February. During the months of March and April, freezing and thawing of soils is a very common

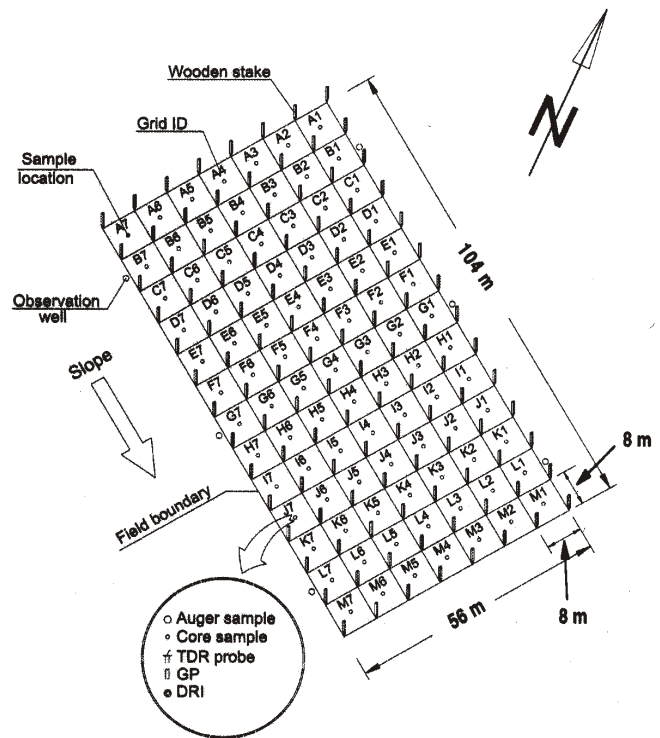


Fig. 2. Experimental set-up in the field.

phenomenon. Based on the climatic characteristics, this regions can be divided into four seasons: summer (June - August), fall (September - December), winter (January-March), and spring (April - May).

The experimental field has a gently sloping topography with an average slope of approximately 6%. The dominant soil in the field is Guelph sandy loam, with 70% sand, 16% silt, and 14% clay. To investigate the spatial variations in hydraulic conductivity, the experimental field was divided into 91 square blocks, 8 x 8 m in size, as shown in Fig. 2. The field was plowed during fall 1999 to remove vegetation and experimental data on hydraulic conductivity were collected during summer 2000.

### EXPERIMENTAL METHODS and ANALYSIS PROCEDURE

Two field techniques, double ring infiltrometer (DRI) and Guelph permeameter (GP), were used to determine the values of  $K_{fs}$  at 91 blocks in the field. The infiltration tests using DRI and steady state infiltration test, using GP, were conducted approximately in the centre of each block. Based on the structure of the technique, the values of  $K_{fs}$  obtained by the DRI method can be characterized as surface values and  $K_{fs}$  values obtained by GP as shallow subsurface values obtained at a depth of 0.2 m (Gupta et al. 1993).

#### Description of double ring infiltrometer method

The DRI consists of two concentric metal rings of 0.305-m (inner ring) and 0.605-m (outer ring) diameter. These rings were carefully inserted into the soil to a depth of 0.15 m. Water was poured into the rings, and a constant head of 0.15 m was maintained within the inside ring throughout the experimental period. Water was also kept in the outer ring to prevent the

lateral movement of water beneath the inner ring, thus maintaining one dimensional flow condition. The amount of cumulative infiltration with time was recorded and subsequently converted to the corresponding infiltration rates for elapsed times from the start of the experiment. The infiltration data obtained were analyzed with the Philip's infiltration equation to determine  $K_{fs}$  values.

Philip (1957) showed that one dimensional infiltration under ponded conditions could be described by a simple and rapidly converging power series in  $t^{1/2}$ :

$$I = At + St^{1/2} \quad (1)$$

where:

- $I$  = cumulative infiltration (m),
- $A$  = parameter known as transmissivity factor (m/s),
- $S$  = sorptivity (m/s<sup>1/2</sup>), and
- $t$  = elapsed time since the start of infiltration (s).

The parameter  $A$  reflects the steady state infiltration rate into the wetting zone, whereas the parameter  $S$  has been interpreted to be the component of infiltration due to vertical gradient in the soil matric potential during the early stages of infiltration. These parameters are functionally related to the  $K_{fs}$ . These parameters were determined by fitting the time derivative of Eq.1 to the collected infiltration data. The intercept of the straight line between ' $dI/dt$ ' and ' $t^{-1/2}$ ' yield was the value of parameter ' $A$ '. The  $K_{fs}$  value was determined by a multiplying parameter  $A$  by a factor of 2/3 (Youngs 1968).

### Description of Guelph permeameter method

The procedure suggested by Reynolds and Elrick (1985) was used to determine  $K_{fs}$  by the GP. This method measures steady state rate of water flow required to maintain a constant depth of water in a 0.15-0.2-m deep cylindrical test hole. The GP method is based on the assumption of three - dimensional steady state infiltration from a cylindrical test hole in unsaturated soil. The permeameter consists of an "in-hole Mariotte bottle" made of two concentric tubes. The inner "air inlet" tube provides the air supply, and the outer tube serves as the water reservoir and as an outlet into the well. Water flows out of the outlet tube through a funnel shaped perforated section located above the permeameter tip.

The permeameter was inserted in a 0.065 m diameter hole, and the air inlet tube was adjusted to maintain a constant depth of water (head) in the hole. The discharge from the permeameter, which was equal to the recharge from the hole into the soil, was monitored at fixed time intervals until a steady state rate was obtained. The procedure was repeated to obtain a steady state discharge rate at a second depth of water head, higher than the first one. Two heights of ponded water in the test hole and their corresponding steady state discharge rates constituted one set of observations to determine  $K_{fs}$ .

In the present study, the data collected were analyzed using Eq. 2 to determine  $K_{fs}$ ,

$$Q = 2\pi H^2 \frac{K_{fs}}{C} + \pi a^2 K_{fs} + 2\pi H \frac{\phi_m}{C} \quad (2)$$

where:

- $Q$  = steady-state recharge (m<sup>3</sup>/s),
- $H$  = depth of water maintained in the auger hole (m),

- $a$  = radius of cylindrical auger hole (m),
- $K_f$  = field saturated hydraulic conductivity (m/s),
- $C$  = shape coefficient, and
- $\phi_m$  = matric flux potential (m<sup>2</sup>/s).

The three terms on the right hand side of Eq. 2 represent the contributions of pressure, gravity, and capillary processes towards the steady-state recharge rate, respectively. The graphical relationships between  $C$  and  $H/a$  ratio developed by Elrick et al. (1987) were used to obtain a value of  $C$  corresponding to the measured head in the test hole.

A computer program, GP\_Cal, developed by Zhang and Parkin (1998) was used to estimate  $K_{fs}$ . Initially, all the computations were performed using two ponded height techniques. This resulted in 60% negative values of  $K_{fs}$ . Therefore, one ponded height technique was used to estimate  $K_{fs}$  for those data points where negative values of  $K_{fs}$  were obtained from the two-head technique. The one-ponded height technique can be used to estimate  $K_{fs}$  only if the site value of  $\alpha$  ( $K_{fs}/\phi_m$ ) is known. For this study the value of ' $\alpha$ ' was obtained from Elrick and Reynolds (1992) and the published value of ' $a$ ' was compared using the values of  $K_{fs}$  obtained with the two-ponded height technique. The computed value of ' $\alpha$ ' as 18 m<sup>-1</sup> was very close to value of ' $a$ ' reported by Elrick and Reynolds (1992). Also, the positive values of  $K_{fs}$  determined by the two-ponded-head technique were compared with values of  $K_{fs}$  determined by one-ponded head technique. These values of  $K_{fs}$  were very close to the values estimated by two-ponded height techniques.

### Description of geostatistical analysis

Conventional statistical techniques such as frequency analysis and analysis of variance (ANOVA) do not consider correlation between measurements taken at different locations. Therefore, geostatistical techniques can be used to analyze the spatial correlation structure of soil physical and hydraulic properties, such as percent sand, silt, and clay, bulk density, effective porosity, organic matter content and saturated hydraulic conductivity (Diiwu et al. 1998; Nielson et al. 1973; Gupta 1993). Geostatistics is based on the science of regional variables. Regional variables are variables which are random in space, i.e. property values at different locations are repeated trials and values are characterized by a probability distribution. In this study, auto-correlation, semi-variogram, and kriging techniques were used to analyze the spatial correlation structure of saturated hydraulic conductivity at the field scale.

### Auto-correlation function

The sample auto-correlation function ( $r_k$ ) was estimated from Eq.3 as given by Warrick and Nielsen (1980):

$$r_k = \frac{C_k}{\sigma_E^2} \quad (3)$$

$$C_k = \left( \frac{1}{n-k-1} \right) \sum_{i=1}^{n-k} (x_i - \sigma_E)(x_{i+k} - \sigma_E) \quad (4)$$

where:

- $k$  = index for separation of  $k$  intervals (lag  $k$ ),
- $C_k$  = auto-covariance,
- $\sigma_E$  = standard deviation, and
- $x_1, x_2, x_3, \dots, x_n$  = values of hydraulic conductivity at different locations.

A plot of the auto-correlation function against the lag number  $k$  is called a correlogram. A correlogram is useful to determine the correlation between successive observations (Haan 1977) and to determine the average distance over which observations are correlated. Interpretation of auto-correlation functions is difficult and sometimes misleading (Jenkins and Watts 1968) because errors arising from estimating one-correlation coefficient are correlated with errors in adjacent coefficients, which makes testing for statistical significance difficult. Therefore, it is preferred to perform spectral analysis to determine periodicity in data. Webster (1977) and Vauclin et al. (1982) have outlined a procedure to analyze data by using the spectral density function  $S(f)$  for a discrete spatial series as:

$$S(f) = \Delta x \left[ r(0) + 2 \sum_{k=1}^m r(k) \cos(2nkf\Delta x) \right] \quad (5)$$

where:  $m$ =maximum number of correlation lags.

The values of  $S(f)$  should be computed only for frequencies given by:

$$f = \frac{k}{m} f_N \quad (6)$$

where:  $f_N$  = the Nyquist frequency =  $\Delta x/2$

### Semi-variogram

Semi-variograms are used to measure the spatial correlation structure. The relationship between semi-variance and distance between the sample pairs is given by:

$$\gamma(h) = \frac{1}{2N(h)} \sum_{j=1}^{N(h)} \left[ Z(x_j) - Z(x_j + h) \right]^2 \quad (7)$$

where:

- $Z(x_j), Z(x_j + h)$  = values of a random variable  $x_j$  and  $x_{j+h}$  respectively,  
 $N(h)$  = number of sample pairs separated by  $h$ ,  
 $h$  = distance between sample values (lag), and  
 $\gamma(h)$  = estimated value of the semi-variance for lag  $h$ .

**Table 1. Summary of statistical analysis of  $K_{fs}$  estimated by double ring infiltrometer (DRI) and Guelph permeameter (GP).**

| Parameter      | DRI (2000)             |               | GP (2000)              |               |
|----------------|------------------------|---------------|------------------------|---------------|
|                | $K_{fs}$               | $\ln(K_{fs})$ | $K_{fs}$               | $\ln(K_{fs})$ |
| Mean           | $2.92 \times 10^{-2}$  | -4.23         | $4.19 \times 10^{-2}$  | -3.72         |
| SD             | $3.25 \times 10^{-2}$  | -3.27         | $4.57 \times 10^{-2}$  | -3.45         |
| Variance       | $10.53 \times 10^{-2}$ | -2.83         | $20.89 \times 10^{-2}$ | -3.28         |
| CV (%)         | 111.30                 | 352.6         | 109.0                  | 130.3         |
| Minimum (m/h)  | $0.05 \times 10^{-2}$  | -7.59         | $0.07 \times 10^{-2}$  | -7.35         |
| Maximum (m/h)  | $13.01 \times 10^{-2}$ | 2.57          | $26.40 \times 10^{-2}$ | -1.33         |
| N* (n missing) | 91 (0)                 | 91 (0)        | 91 (0)                 | 91 (0)        |
| Skewness       | 1.51                   | -0.44         | 2.34                   | -0.57         |
| Kurtosis       | 1.43                   | -0.32         | 6.71                   | 0.34          |

\*Number of data points

If the semi-variogram changes with direction, the spatial variation is said to be anisotropic and a transformation is required before the semi-variogram can be used for kriging. Various variogram model functions are available in the literature to represent the structure of a set of data (Isaaks and Srivastava 1989). The most common models are linear, spherical, gaussian, and exponential. The exponential model was used to represent the structure of the  $K_{fs}$  data, as the exponential model fits well to the experimental variogram as compared to other models in this study.

### Kriging

Semivariograms are applied to calculate the best linear unbiased estimate at locations where no measurements are available. The technique is called kriging and a kriged estimate of the variable at location  $x_0$  is given by:

$$Z^*(x_0) = \sum_{i=1}^n w_i Z(x_i) \quad (8)$$

where:

- $n$  = number of locations where measurements are made,  
 $Z(x_i)$  = measurements selected in the  $x_0$  neighborhood for performing the estimation of  $Z^*(x_0)$ ,  
 $Z^*(x_0)$  = kriging estimate at location  $x_0$ , and  
 $w_i$  = weights associated with the distance between  $x_0$  and  $x_i$ .

The following two conditions are required for computation of  $w_i$ :

- (i) Nonbias condition :  $E[Z^*(x_0) - Z(x_0)] = 0$   
(ii) Condition of minimum estimation variance given in expected value notation as to minimize  $E[Z^*(x_0) - Z(x_0)]^2$

## RESULTS and DISCUSSION

In this study, all of the above mentioned methods were used to study the spatial variations of  $K_{fs}$  along and across the slope of an experimental field.

### Statistical analysis

Table 1 shows the statistics summary on  $K_{fs}$  obtained by the DRI and GP during summer 2000. The values of  $K_{fs}$  for DRI ranged from  $0.05(10^{-2})$  to  $13.01(10^{-2})$  m/h with a mean of  $2.92(10^{-2})$  m/h and  $0.07(10^{-2})$  to  $26.40(10^{-2})$  m/h with a mean of  $4.19(10^{-2})$  m/h for GP. The statistical analysis indicates that the mean value of  $K_{fs}$  obtained by DRI is 44% greater than the mean value obtained by GP. The coefficient of variation (CV) for  $\ln(K_{fs})$  values is 353% for DRI, which was 2.7 times the obtained from GP technique. The values of mean and CV are well within an order of magnitude reported in the literature (Nielson et al. 1973; Sisson and Weirenga 1981; Vierra et al. 1981; Jury 1989; Kanwar et al. 1989)

The possible reason for the higher values of mean and CV of  $K_{fs}$  for DRI could be attributed to the experimental constraints associated with the DRI method. Though every possible precaution was taken

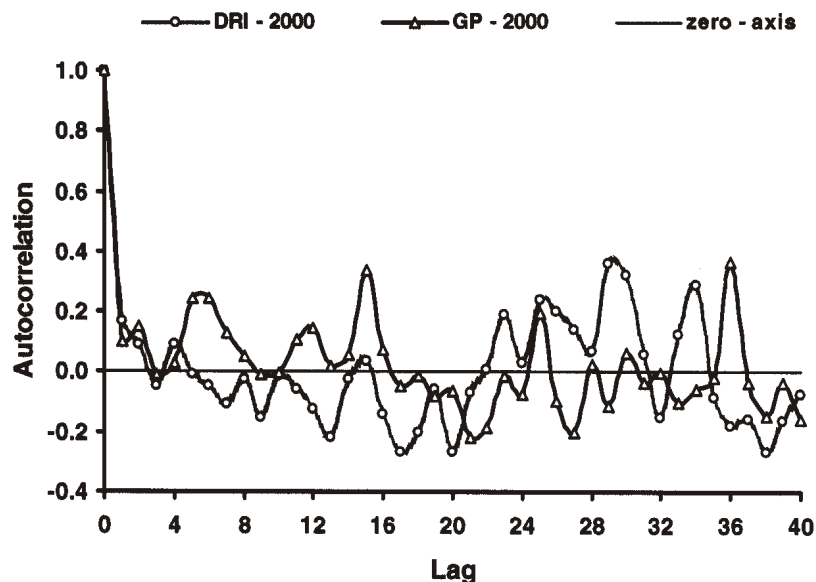


Fig. 3. Correlogram of field saturated hydraulic conductivity ( $K_{fs}$ ) along the field slope.

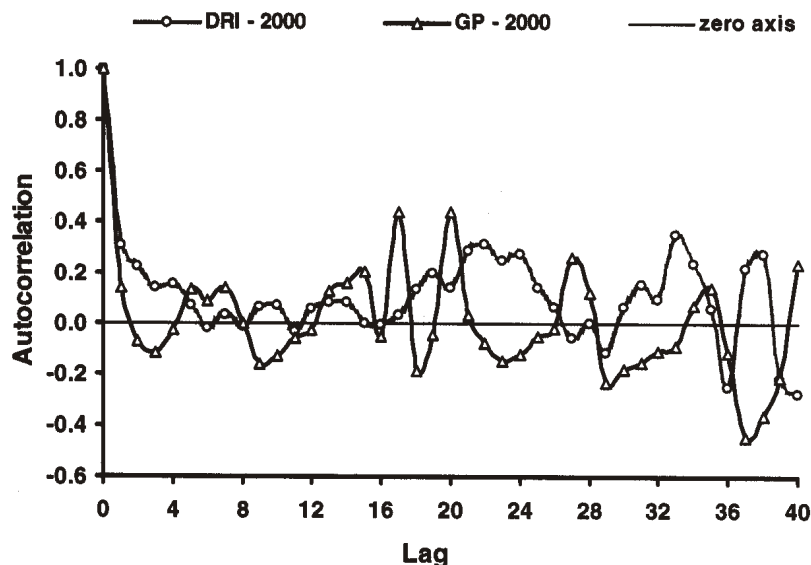


Fig. 4. Correlogram of field saturated hydraulic conductivity ( $K_{fs}$ ) across the field slope.

to simulate one-dimension steady state flow under constant water head ponding conditions, it is possible that freezing and thawing of soil during the spring period and biological activities may have created pathways for lateral movement of infiltrating water away from the infiltrometer rings. Rapid infiltration of water and the escape of air bubbles from the soil surface observed during DRI experiments indicate that the soil was disturbed and loose at the time of the experiment. Under such conditions, it was very difficult to maintain a precise constant head over the surface area covered by the inner ring of the infiltrometer at some experimental locations in the field.

The lower value of coefficient of variation for the GP method could be due to the nature of the method itself. The GP method is based on a steady-state, three-dimensional infiltration

from a well-source in unsaturated soil. The solution reflects the combined effects of pressure, gravity, and capillary flows on steady-state recharge in an approximate spherical-shaped soil volume. The GP estimated  $K_{fs}$  at a depth of approximately 0.2 m in an auger hole of 0.06-m diameter and the soil was less disturbed at the subsurface as compared to the surface. Though every possible precaution was taken in preparing the auger hole, smearing of the well wall may also have added to the variation in hydraulic conductivity values.

#### Geostatistical analysis

The spatial variability of hydraulic conductivity was also determined with geostatistical techniques including correlogram, power spectrum, and kriging. Also, the correlation scale or integral scale of the hydraulic conductivity was calculated from a correlogram drawn along and across the slope of the field. Basically, the integral scale represents the average dimension of the heterogeneity (Yeh 1998). Very little information is available on the correlation scale of soil properties with respect to the direction of slope. Therefore, the correlation scale was calculated for the hydraulic conductivity from a correlogram drawn along and across the slope of the experimental field.

#### Correlogram

A correlogram is a plot between auto-correlation and lag distance. Correlograms were drawn up to 50 lags to observe variations in the data. The auto-correlation has a maximum value of '1' at zero lag, then decreases to zero as lag distance increases. A detailed description of the auto-correlation up to 50 lags for  $K_{fs}$  along and across the slope of the experimental field is shown in Figs. 3 and 4, respectively.

At a distance of 20 and 24 m, the auto-correlation was zero for DRI and GP data, as shown in Fig. 3, indicating that samples beyond this distance are independent. Basically, this distance represents the range of a semi-variogram. The correlogram of GP exhibits less variation as compared to DRI, indicating that  $K_{fs}$  exhibits less spatial variability in the subsurface than at the surface. The integral scale estimated from the correlogram for DRI and GP was 6.5 m which indicates that in-situ field measurements can be made at the same distance using DRI and GP along the slope of a field.

Figure 4 represents the correlogram for DRI and GP data across the slope of the field. The correlogram across the slope exhibits less variation than the correlogram along the slope indicating that  $K_{fs}$  across the slope of the field was less spatially variable than along the slope of field. At distances of 18 and 48 m, the auto-correlation was zero for GP and DRI, respectively. The value of the integral scale estimated from a correlogram across the slope was 8.0 m and 7.0 m for DRI and

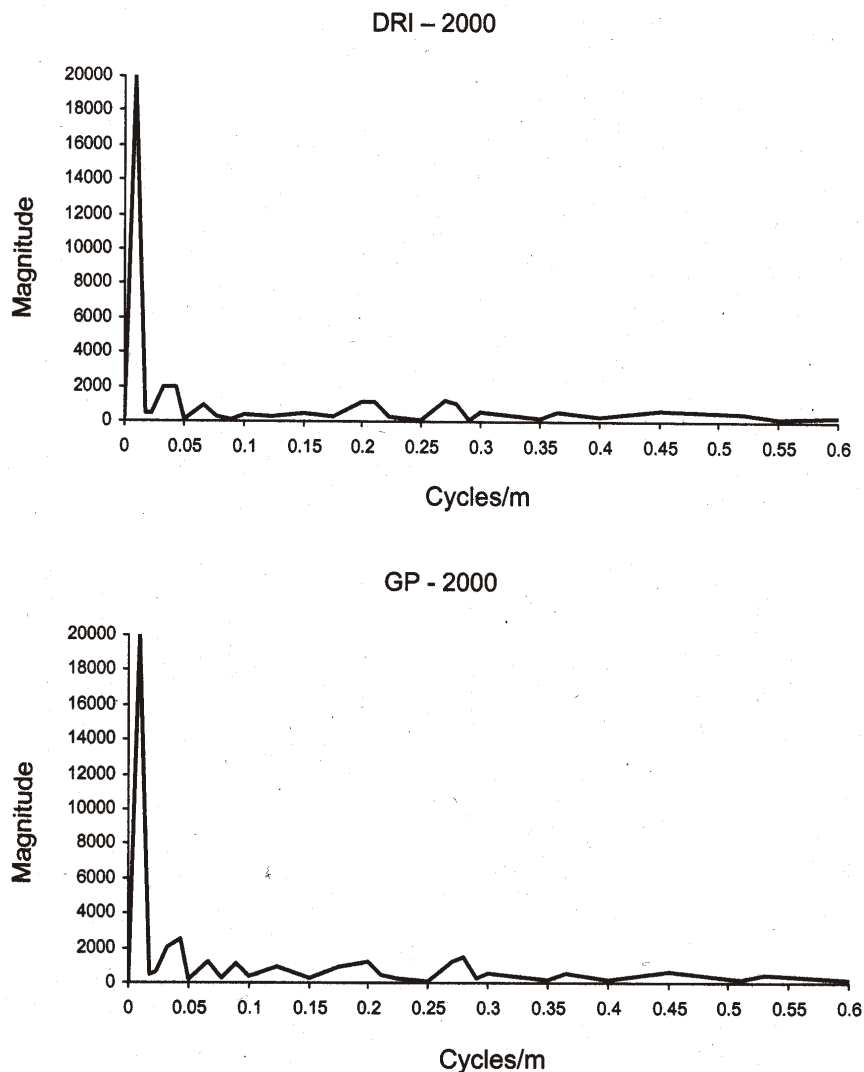


**Fig. 5. Power-spectrum of field saturated hydraulic conductivity ( $K_{fs}$ ) determined by double ring infiltrometer (DPI) and Guelph permeameter (GP).**

GP data, respectively. The average value of the integral scale, across the slope, was 8.0 m which was 23% greater than the integral scale along the slope of the field. It reveals that the spatial variability was more along the slope of the field than across the slope. These differences in spatial variability may be due to the detachment of soil from the ridges and deposition in the valleys. This suggests that the approach adopted to obtain a true preventative value of hydraulic conductivity requires a shorter sampling interval along the slope than across the slope.

The graphical information obtained from the correlogram was also used to determine the trend in the spatial structure of  $K_{fs}$ . The correlogram for  $K_{fs}$  along and across the slope of field for DRI and GP show some cyclic variations with noise. The cyclic variation in the correlogram for  $K_{fs}$  was confirmed by spectral analysis. Figure 5 shows the power spectrum of  $K_{fs}$  for the DRI and GP data; however the power spectrum shows a very weak periodicity. It is very clear from the correlogram that a Fourier series at different harmonics can be used to represent the spatial variations of  $K_{fs}$  as reported by Gupta et al. (1993).

**Table 2. Model parameters used in kriging procedure.**

| Structure           | Year - 2000 |      |
|---------------------|-------------|------|
|                     | DRI         | GP   |
| Model*              | Exp         | Exp  |
| Direction           | Omni        | Omni |
| Range parameter (m) | 94.2        | 9.8  |
| Sill                | 2.6         | 1.4  |
| Nugget              | 1.32        | 0.34 |
| R <sup>2</sup>      | 0.82        | 0.86 |

\*Exp = Exponential model

### Semi-variogram

A semi-variogram was used for kriging analysis to plot spatial variations of  $K_{fs}$  over an area and to estimate values of  $K_{fs}$  at unsampled locations. A geostatistical software (GS+, Version 3.11, Gamma Design Software, Plainwell, MI) was used to analyse the spatial structure of the  $K_{fs}$  for DRI and GP data. An isotropic and anisotropic empirical semi-variogram in the east - west (along the slope) and north - south (across the slope) direction were calculated for DRI and GP data and the results are presented in Fig. 6.

The shapes of the semi-variogram of  $K_{fs}$  for DRI and GP data are similar; however, the semi - variance for each lag value is higher for DRI than GP. An exponential model was also fitted to the experimental semi-variogram for DRI and GP data and the parameters of the fitted exponential model is presented in Table 2. These results indicate that  $K_{fs}$  obtained from DRI was more spatially variable than  $K_{fs}$  determined by using GP. Similarly, the semi-variogram calculated for the east-west direction is positioned above the

north-south directional semi-variogram. Such a trend indicates that spatial variability of  $K_{fs}$  is also associated with direction. Also a high value of nugget for the empirical semi-variogram for DRI and GP data indicates that  $K_{fs}$  is highly spatially variable within a sample volume. The empirical semi-variogram of  $K_{fs}$  obtained from DRI shows a poor spatial structure, indicating that  $K_{fs}$  measurements were not correlated to each other. However, the empirical semi-variogram for GP data shows a better spatial structure than DRI data indicating that  $K_{fs}$  measurements made at a distance of 20 m or less are highly correlated to each other. The analysis also indicates a very small difference between the directional and omni-directional (isotropic) semi-variograms of  $K_{fs}$ . Therefore, isotropic semi-variograms are used for kriging analysis to estimate values of  $K_{fs}$  at unsampled locations for DRI and GP.

### Kriging

The parameters of the exponential model fitted to the experimental variogram were used in the kriging process to provide the estimate of  $K_{fs}$  at unsampled locations. Maps of the

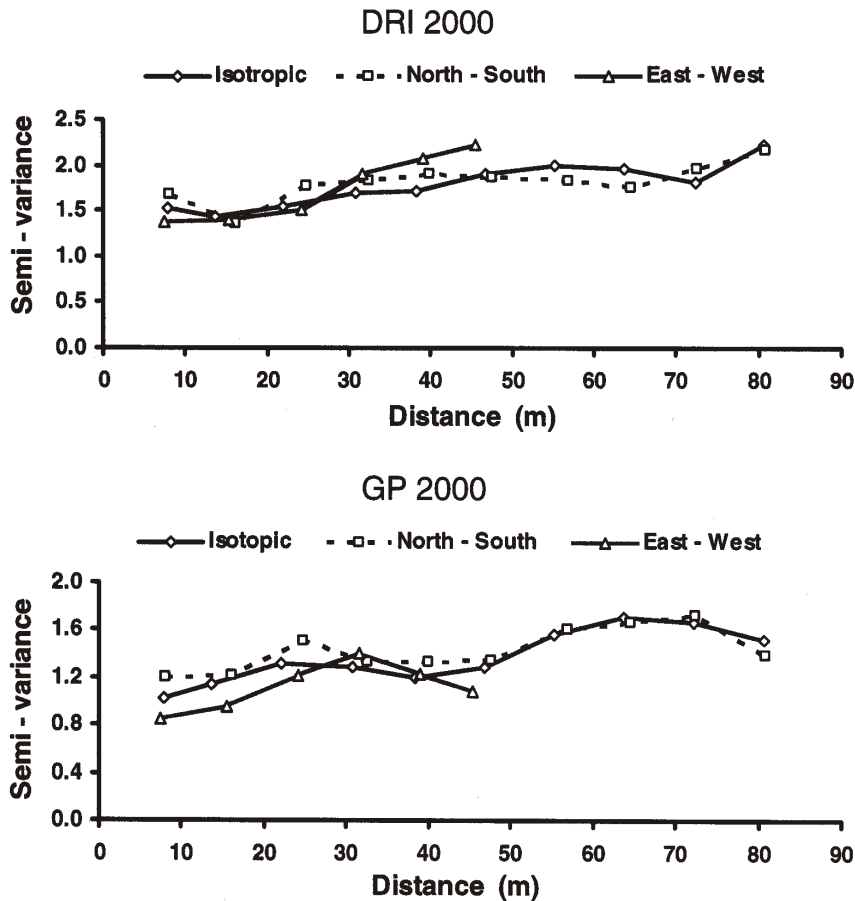


Fig. 6. Empirical variogram of field saturated hydraulic conductivity ( $K_{fs}$ ) determined by double ring infiltrometer (DPI) and Guelph permeameter (GP).

kriged estimates provided a visual representation of the arrangement of the population and were used to interpret the spatial and temporal variations in  $K_{fs}$ . Block kriging was performed with a search radius of 20 m and 12 numbers of neighbors. Kriging estimates of  $K_{fs}$  and standard deviations were made on a 2 x 2 m grid. The contour maps obtained from this analysis are presented in Fig. 7. The contour maps of  $K_{fs}$  for DRI and GP exhibit a distinct pattern. The directional trends in  $K_{fs}$  are clearly visible as elliptical shapes extending from east to west, across the slope of field. This trend also indicates that spatial variation in  $K_{fs}$  is larger along the slope of the field as compared to across the slope of the field. A similar trend was observed in the correlation scale analysis. The correlation scale was 20% higher along the slope of the field indicating that soil samples should be taken at a smaller spatial interval along the slope of field to represent a true population of the data. The analysis of contour plots of  $K_{fs}$  in the light of other soil properties may have potential to identify runoff generation areas and dominant runoff generation mechanisms.

### CONCLUSIONS

The application of conventional statistics and geo-statistical techniques indicate that saturated hydraulic conductivity of soil is a highly spatially variable soil property. The geo-statistical approaches describe the spatial variability better than the conventional

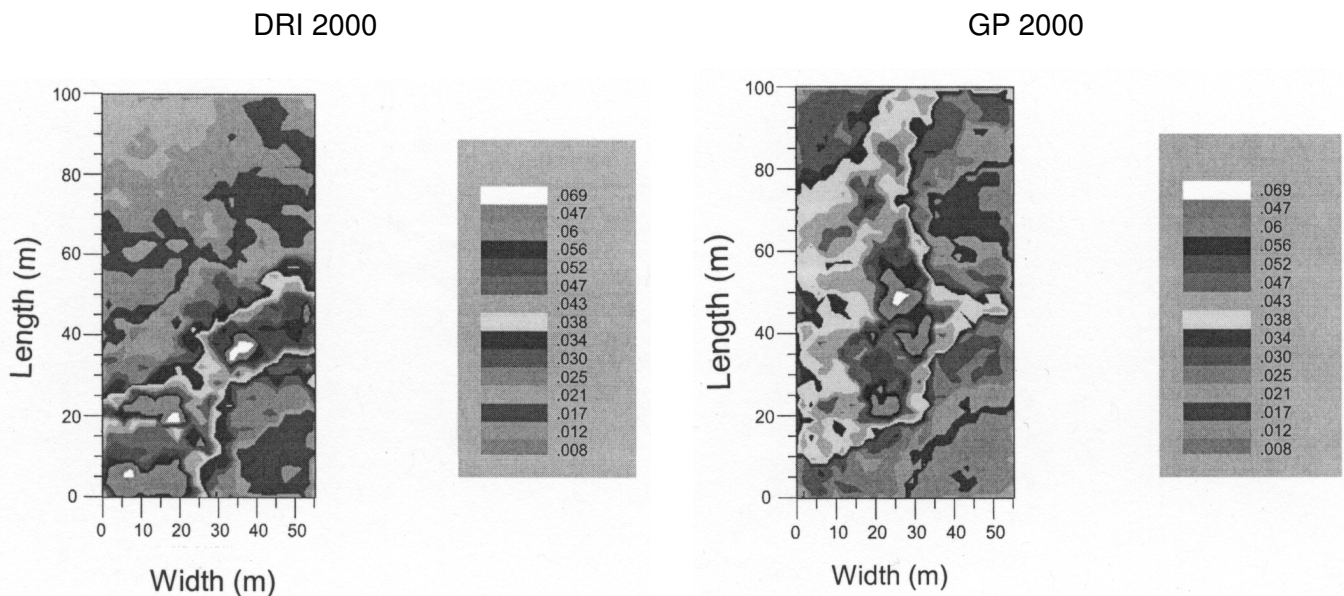


Fig. 7. Kriged map of field saturated hydraulic conductivity ( $K_{fs}$ ) determined by double ring infiltrometer (DPI) and Guelph permeameter (GP).

statistical approaches. The saturated hydraulic conductivity exhibits more spatial variation along the field slope than across the field slope, therefore, a shorter sampling interval is required along the slope than across the slope to obtain true representative values of hydraulic conductivity at a field scale. A kriging procedure produces convenient smooth hydraulic conductivity surfaces that may be useful for estimating values of saturated hydraulic conductivity at unsampled locations.

## REFERENCES

- Buchter, B., P.O. Aina, A.S. Azari and D.R. Nielsen. 1991. Soil spatial variability along transects. *Soil Technology* 4:297-314.
- Diiwu, J.Y., R.P. Rudra, W.T. Dickinson and G.J. Wall. 1998. Effect of tillage on the spatial variability of soil water properties. *Canadian Agricultural Engineering* 40(1): 1-7.
- Elrick, D.E. and W.D. Reynolds. 1992. Methods for analyzing constant head well permeameter data. *Soil Science Society of America Journal* 56(1):320-323.
- Elrick, D.E., W.D. Reynolds, N. Baumgartner, K.A. Tan and K.L. Bradshaw. 1987. In-situ measurement of hydraulic properties of soils using the Guelph Permeameter and Guelph Infiltrometer. In *Proceedings Third International Symposium on Land Drainage*, 13-23. Columbus, Ohio: Ohio State University.
- Govindaraju, R.S., J.K. Koelliker, A.P. Schwab and M.K. Banks. 1995. Spatial variability of surface infiltration properties over two fields in the Konza Prairie. Poster presented at the Hazardous Waste Research Conference, Manhattan, KS.
- Gupta, R.K. 1993. Modeling soil water flow process using stochastic approach. Unpublished Ph.D. thesis. Guelph, ON: School of Engineering, University of Guelph.
- Gupta, R.K., R.P. Rudra, W.T. Dickinson, N.K. Patni and G.J. Wall 1993. Comparison of saturated hydraulic conductivity measured by various field methods. *Transactions of the ASAE* 36: 51-55.
- Hann, C.T. 1977. *Statistical Methods in Hydrology*, 1st edition. Ames, IA: The Iowa State University Press.
- Isaaks, E.H. and R.M. Srivastava 1989. *An Introduction to Applied Geo-statistics*. New York, NY: Oxford University Press.
- Jenkins, G.M. and D.G. Watts 1968. *Spectral analysis and its applications*. London, UK: Holden-Day Series in Time Series Analysis.
- Jury, W.A. 1989. Chemical movement through soil. In *Vadose Zone Modelling of Organic Pollutants*, eds. S.C. Hern and M.S. Melacon, 135-139. Chelsea, MI: Lewis Publishing Inc.
- Kanwar, R.S., H.A. Rizvi, M. Ahmed, J.R. Horton and S.J. Marley. 1989 A comparison of two methods for rapid measurement of saturated hydraulic conductivity of soils. *Transactions of the ASAE* 2(2):1885-1891.
- Klute, A. 1965. Laboratory measurement of hydraulic conductivity of saturated soil. In *Methods of Soil Analysis*, Part 1, ed. C.A. Black, 210-221. Monograph No. 9, Madison, WI: American Society of Agronomy.
- Mohanty, B.P., M.D. Ankeny, R. Horton and R.S. Kanwar. 1994. Spatial analysis of hydraulic conductivity measured using disc infiltrometer. *Water Resources Research* 30(9):2489-2498.
- Nielson, D.R., J.W. Biggar and K.T. Erh. 1973. Spatial variability of field measured soil water properties. *Hilgardia* 42(7):215-259.
- Philip, J.R. 1957. The theory of infiltration: The infiltration equation and its solution. *Soil Science* 83:345-357.
- Rahman, S., L.C. Munn, R. Zhang and G.F. Vance. 1996. Wyoming Rocky Mountain forest soils: Evaluating variability using statistics and geostatistics. *Canadian Journal of Soil Science* 75:501-507.
- Rawls, W.J., D.L. Brakensick and K.E. Saxton. 1982. Estimation of soil water properties. *Transactions of the ASAE* 25: 1316-1320.
- Reynolds, W.D. and D.E. Elrick 1985. In-situ measurements of field saturated hydraulic conductivity, sorptivity and alpha parameter using the Guelph Permeameter. *Soil Science* 140(4): 292-302.
- Rudra, R.P., W.T. Dickinson and G.J. Wall 1985. Application of CREAMS model in southern Ontario conditions. *Transactions of the ASAE* 28(4):1233-1240.
- Sisson, J.B. and P.J. Weirenga 1981. Spatial variability of steady state infiltration rates as a stochastic process. *Soil Science Society of America Journal* 45:699-704.
- Stephens, D.B., S. Tyler and D. Watson. 1984. Influence of entrapped air on field determination of hydraulic properties in the vadose zone. In *Proceedings of Conference on Characterization and Monitoring in the Vadose Zone*, 57-76. Worthington, OH: National Water Well Association.
- Vauclin, M., S.R. Vieira, R. Benara and J.L. Hatfield. 1982. Spatial variability of surface temperature along two transects of a bare soil. *Water Resources Research* 18(6): 1677-1686.
- Vieira, S.R., D.R. Nielsen and J.W. Biggar 1981. Spatial variability of field measured infiltration rate. *Soil Science Society of American Proceedings* 32:1040-1048.
- Warrick, A.W. and D.R. Nielson 1980. Spatial variability of soil physical properties in the field. In *Applications of Soil Physics*, ed. D. Hillel, 319-344. New York, NY: Academic Press, Inc.
- Webster, R. 1977. Spectral analysis of Gilgai soil. *Australian Journal of Soil Research* 15:191-204.
- Webster, R. and M.A. Oliver. 2001. *Geostatistics for Environmental Scientists*. London, UK: John Wiley and Sons Ltd.
- Willardson, L.S. and R.L. Hurst. 1965. Sample size estimated in permeability studies. *Journal of Irrigation and Drainage Engineering*, ASCE 91:1-9.
- Youngs, E.G. 1968. An estimation of sorptivity for infiltration studies from moisture considerations. *Soil Science* 106: 157-163.
- Yeh, T.C.J. 1998. Scale issues of heterogeneity in vadose zone hydrology. In *Scale Dependence and Scale Invariance in Hydrology*, ed. G. Sposito, Chapter 8, 224-265. Cambridge, UK: Cambridge University Press.
- Zhang, Z. and G.W. Parkin. 1998. Guelph permeameter GP\_Cal. Unpublished Report. Department of Land Resource Science, University of Guelph, Guelph, ON.